Journal of Applied Polymer Science

Synthesis and Characterization of Nanosilica/Waterborne Polyurethane End-Capped by Alkoxysilane Via a Sol-Gel Process

Lanlan Zhai,[1] Ruowang Liu,[1] Feng Peng,[1] Yunhao Zhang,[1] Kai Zhong,[1] Jixin Yuan,[2] Yunjun Lan[1]

[1]Key Laboratory of Leather Engineering of Zhejiang Province, College of Chemistry and Materials Engineering, Wenzhou University, Wenzhou 325027, People's Republic of China

[2]Institute of Science and Technology Information of Zhejiang Province, Hangzhou 310006, People's Republic of China

Correspondence to: Y. Lan (E-mail: lanbo3611@163.com)

ABSTRACT: A novel method was used to synthesis nanosilica/waterborne polyurethane (WPU) hybrids by *in situ* hydrolysis and condensation of tetraethyl orthosilicate (TEOS) and/or 3-aminopropyltriethoxylsilane bonding at the end of the WPU molecular chain. The hybrid was characterized by scanning electron microscopy, energy dispersive spectroscopy (EDS), transmission electron microscopy, Fourier transform infrared spectroscopy (FTIR), and X-ray photoelectron spectroscopy (XPS). The results showed that the nanosilica/WPU hybrids with well-dispersed nanosilica particles were synthesized, in which the particles had typical diameters of about 50 nm. In addition, XPS and FTIR analyses demonstrated that chemical interaction occurred between WPU and silica. The effects of TEOS on surface wettability, water resistance, mechanical strength, and thermal properties of the hybrid were also evaluated by contact angle measurements, water absorption tests, mechanical tests, and differential scanning calorimetry, respectively. An increase in advancing contact angles, water resistance, and tensile strength, as well as decrease in elongation at break and glass transition temperature, were obtained with the addition of TEOS. Water absorption decreased from 17.3 to 5.5%. The tensile strength increased to a maximum of 29.7 MPa, an increase of about 34%. Elongations at break of the hybrids decreased 191%. These results were attributed to the effects of the nanosilica and the chemical interaction between WPU and silica. © 2012 Wiley Periodicals, Inc. J. Appl. Polym. Sci. 000: 000–000, 2012

KEYWORDS: polyurethanes; silicas; structure-property relations; mechanical properties; microscopy

Received 21 September 2011; accepted 20 June 2012; published online
DOI: 10.1002/app.38225

INTRODUCTION

Waterborne polyurethane (WPU) has recently emerged as an important alternative to its solvent-based counterparts for various applications because of increasing health and environmental awareness.[1] However, the inferior properties of WPU, such as low mechanical strength and water resistance hindered its wide application. Recently, nano-SiO_2/WPU hybrid materials have evoked intense research interest for the synergetic combination of the properties typical of each of the inorganic and polymer moieties.[2–5]

It is well-known that the dispersion behavior of nano-SiO_2 particles significantly affects the properties of nano-SiO_2/WPU hybrids due to the high surface energy. Moreover, the level of the matrix reinforcement markedly depends on the extent of interaction between the organic and inorganic phases. Therefore, it is important to recognize that dispersion and interfacial interaction of hybrid materials are the decisive factors affecting the properties of the resulting materials.[6] Several methods have been used to prevent nanoparticles from agglomerating and phase separation with polymer,[7] such as surface modification of nanosilica,[8] blending, sol-gel process,[9] *in situ* polymerization, ultrasonication.[10] However, the interactions between organic and inorganic phases are physical interactions.[11,12] As a result, agglomeration or phase separation still exists. Currently, to achieve strong interaction between nano-SiO_2 and WPU, the reported method is the use of both silane coupling agents (SCA) and sol-gel process. Wang et al.[2] and Jeon et al.[5] synthesized nanosilica/WPU hybrid by dispersing commercial hydrophilic silica into WPU prepolymer with one side terminated by 3-aminopropyltriethoxylsilane (APTES). The ethoxy groups of APTES at the end of the molecular WPU chains were hydrolyzed to give silanol groups, which subsequently condensed on the nanosilica to form siloxane. In addition, trifunctional crosslinker was adopted to increase the crosslinking density of the hybrids by Wang et al.[2] It was reported the interaction between silica and WPU macromolecular chains was hydrogen bonding. Lee et al.[8] synthesized UV curable WPU/silica nanocomposites

Applied Polymer SCIENCE

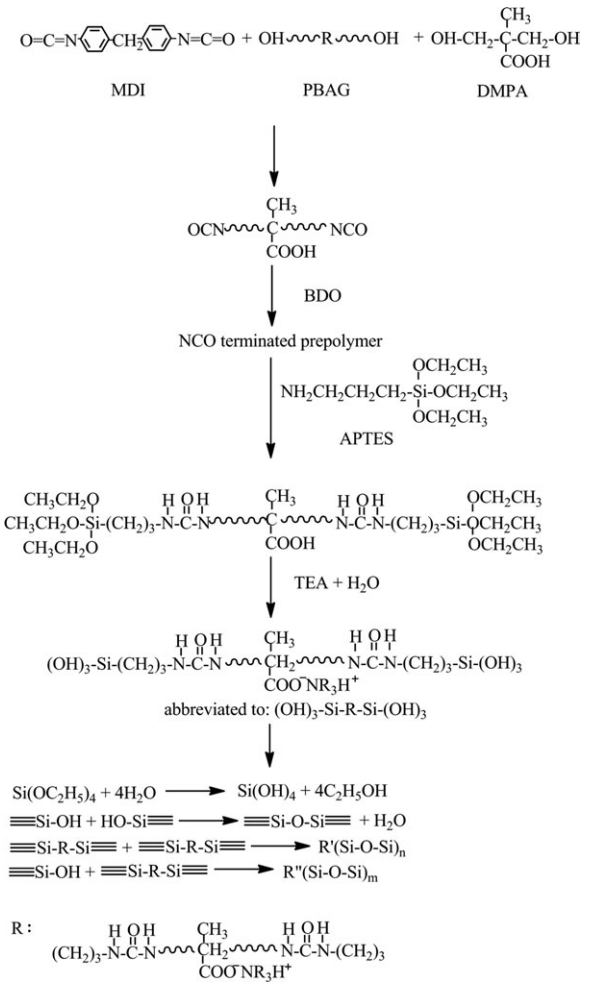

Scheme 1. Reaction route of nanosilica/WPU hybrid composite end-capped by APTES via the sol-gel process.

with functionalized silica particles, which were chemically modified with allyl isocyanates. Silica was incorporated into the WPU by covalent bond. While the compatibility and dispersion of nano-SiO_2 in WPU film was not investigated by them.

To obtain WPU hybrid materials with a uniform dispersion and good compatibility of nano-SiO_2, this study presents an approach to *in situ* synthesize nanosilica/WPU hybrids by simultaneously introducing tetraethyl orthosilicate (TEOS) and APTES into WPU via a sol-gel process. Theoretically, compared to the commercial nanosilica used in those experiments,[2,5,8,9] the nanosilica was synthesized *in situ* in WPU emulsion, where nanosilica was dispersed more evenly. And the process is rather immediate and simple. In this study, the interactions between silica and WPU macromolecular chains are expected to be chemical bonds formed by the reactions of APTES with the isocyanate groups (NCO groups) of the WPU prepolymer and a sol-gel process of APTES with TEOS. Without an external crosslinker, the crosslinking density between nanosilica and WPU is to be improved by APTES and TEOS, which are multifunctional in terms of reactive ethoxy groups and able to form a multidimensional chemical bonding between nanosilica and WPU polymer molecules. This approach also assumes that APTES can improve the dispersion of nanosilica in WPU and the compatibility between nanosilica and WPU. The nanosilica/WPU hybrid materials are then characterized by scanning electron microscopy (SEM), energy dispersive spectroscopy (EDS), transmission electron microscopy (TEM), X-ray photoelectron spectroscopy (XPS), and Fourier transform infrared spectroscopy (FTIR). The effects of TEOS on the surface wettability, water resistance, mechanical strength, and thermal properties of the hybrid materials are also evaluated by contact angle measurement, water absorption tests, mechanical tests, and differential scanning calorimetry (DSC), respectively.

EXPERIMENTAL

Materials

TEOS, absolute ethanol (99.9%), 1,4-butane diol (BDO), and triethylamine (TEA) were purchased from Sinopharm Chemical Reagent (Shanghai, China). 4,4'-Diphenylmethane diisocyanate (MDI) and poly(butylene adipate) glycol (PBAG) were supplied by HuaFon Industrial Group (Zhejiang, China). Dimethylol propionic acid (DMPA) and APTES were purchased from Aladdin Reagent (Shanghai, China). Acetone (98%, Sinopharm Chemical Reagent) was dried over 4-Å molecular sieve before use. All other reagents were used as received.

Samples Preparation

Synthesis of Nanosilica/WPU Hybrid. A mixture of PBAG (M_n = 2000 g mol^{-1}) and DMPA was placed into a 500-mL round-bottom, four-necked separable flask equipped with a mechanical stirrer, nitrogen inlet, thermometer, and condenser. The mixture was stirred, and the water was evaporated at reduced pressure at 110°C in an oil bath for 1 h. MDI was added when the mixture had cooled to 80°C under a nitrogen atmosphere, and the reaction mixture was stirred for 3 h. After cooling to 40°C, BDO and acetone were fed into the reactor, and the mixture was stirred for an additional 2 h. APTES was then slowly added, and the reaction continued for further 1 h, yielding an APTES-terminated prepolymer. Some acetone was added to the mixture to decrease its viscosity. TEA was also added to the flask for neutralization, and the reaction was continued for 0.5 h with stirring. Later, different weight percentages of TEOS and deionized water were added with vigorous stirring for another 2 h, and the acetone was removed. Finally, a homogeneous solution with a solid hybrid content of 30 wt % was obtained. The solution was cast onto a Teflon pan and dried in a programmable temperature-controlled oven for 48 h at 80°C to produce a hybrid film. The reaction scheme, the schematic structure, and the recipes of nanosilica/WPU hybrid composites are shown in Schemes 1 and 2, and Table I, respectively.

Synthesis of WPU. WPU was also prepared for comparison. The process was similar to the one above, except that BDO was added to the reaction mixture without APTES or TEOS. The reaction scheme is shown in Scheme 3. The film was prepared according to the method mentioned in Synthesis of Nanosilica / WPU Hybrid.

Characterization

Morphological analysis of the hybrids was undertaken using SEM (FEI Nova NanoSEM 200). The samples were freshly

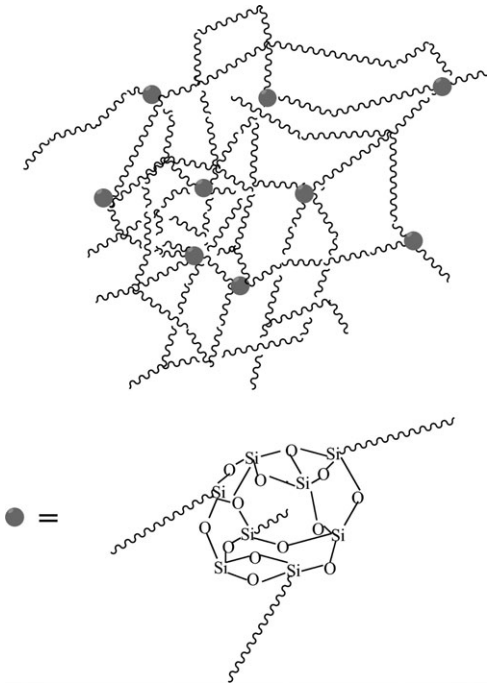

Scheme 2. Schematic structure of nanosilica/WPU hybrid composite end-capped by APTES via the sol-gel process.

broken in liquid nitrogen and the cross-sections were coated by gold sputtering. EDS coupled with SEM was used to analyze the chemical composition of the particles synthesized by this method.

TEM micrographs were taken with a Hitachi H-800 apparatus (Hitachi, Japan). Samples were prepared by an ultramicrotome at low temperature and collected by carbon-film-supported copper grids, giving nearly 100-nm thick sections.

XPS (Axis Ultra Dld, Kratos) was used to investigate the chemical states of the films. The spectra were recorded with monochromatized Al (mono) Kα radiation (1486.6 eV) as the excitation source and a base pressure of 3.6×10^{-9} mbar at a constant power of 120 W (15 kV, 8 mA). The pass energies were 160 (for survey spectra) and 20 eV (for high resolution spectra), and all the peaks were calibrated using C1s at 284.60 eV as the reference.

An FTIR spectrometer (PerkinElmer) was used to characterize the chemical binding of the nanosilica/WPU hybrid and WPU films.

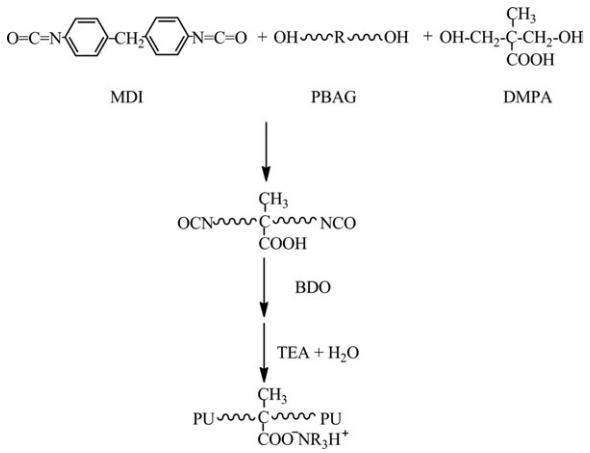

Scheme 3. Reaction route of WPU.

Contact angles were measured by a dynamic contact angle meter and tensiometer (DCAT 11, Dataphysics Instruments GmbH, Filderstadt, Germany). The data were automatically processed using SCAT 32 software. A sample film was held in a special sample holder and then immersed into water. The speed of the lift motor was 0.2 mm/s. In the loop, the weight difference was continuously recorded by the electrobalance, and the contact angle was calculated based on the Wilhelmy method. Five immersion-emersion cycles were carried out for each specimen, and each run was repeated three times for all the film samples.

The degree of water absorption was measured by preserving a test film in water for 24 h and calculating using the following equation:

Degree of water absorption % $= (W - W_0)/W_0 \times 100\%$, where W_0 and W represent the film weights before and after water absorption, respectively. For each hybrid film with different TEOS contents, at least six measurements were conducted.

Mechanical property tests were performed by using a Universal Testing Machine (Shenzhen Reger Instrument, China). The specimens were dumbbell-cut from the film, the schematic diagram of which is shown in Figure 1. The crosshead speed was 100 mm·min^{-1}. A 20-mm benchmark and the original cross-sectional area were used to calculate the mechanical properties. Tests were conducted at room temperature, and the average of at least six measurements for each sample was reported.

The thermal properties were measured with a DSC analysis Q-400 system (TA Instrument, USA) in a nitrogen atmosphere. All

Table I. Recipes for the Preparation of Nanosilica/WPU Hybrid Composites

Sample designation	MDI (mol)	PBAG (mol)	DMPA (mol)	BDO (mol)	APTES (mol)	TEA (mol)	TEOS (wt %)
WPU0	0.039	0.01	0.013	0.009	0	0.013	0
WPU2.5	0.039	0.01	0.013	0.007	0.0045	0.013	2.5
WPU5	0.039	0.01	0.013	0.007	0.0045	0.013	5.0
WPU7.5	0.039	0.01	0.013	0.007	0.0045	0.013	7.5
WPU10	0.039	0.01	0.013	0.007	0.0045	0.013	10.0

Applied Polymer SCIENCE

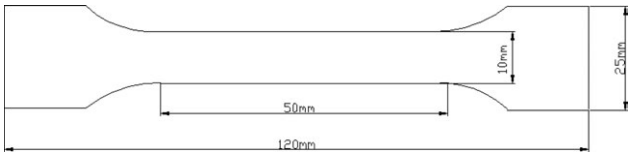

Figure 1. Schematic diagram of the samples for mechanical properties measurement.

samples were scanned over the temperature range from −80 to 200°C at a heating rate of 10°C min^{-1}.

RESULTS AND DISCUSSION

Morphology and Chemical Composition Characterization

The fractured surface morphologies of nanosilica/WPU hybrids and WPU were observed via SEM. The SEM micrographs show that nanoparticles were synthesized in the hybrids [Figure 2(a–c)], whereas no particles appeared in Figure 2(d). The particles were homogeneously dispersed in WPU matrix and there was no particle aggregation in WPU matrix as the TEOS contents increased from 2.5 to 10 wt %. The particles with different TEOS contents showed similar diameters, less than 100 nm from Figure 2(a–c). These implied that the TEOS contents had little influence on the size and dispersion of the particles. EDS results of the nanoparticles in the hybrid films with different TEOS contents [Figure 3(a–c)] demonstrate that the particles were composed of Si and O. The Si/O molar ratio of the nanoparticles in the hybrid films was 33/67, which is equal to the stoichiometric ratio of Si/O in SiO_2, suggesting that the nanoparticles in the hybrid films with different TEOS contents were SiO_2. SiO_2 in the WPU matrix is believed to originate from *in situ* hydrolysis and condensation of TEOS and/or APTES bonding at the end of WPU molecule chains.

Nanoparticles Dispersion in Hybrid Film

TEM micrographs of nanosilica/WPU hybrid films with different TEOS contents are shown in Figure 4. Compared the TEM micrographs of WPU2.5, WPU5, and WPU10 (Figure 4), the amount of nanosilica (dark spheres) increased obviously as the contents of TEOS increased. The particles without aggregation

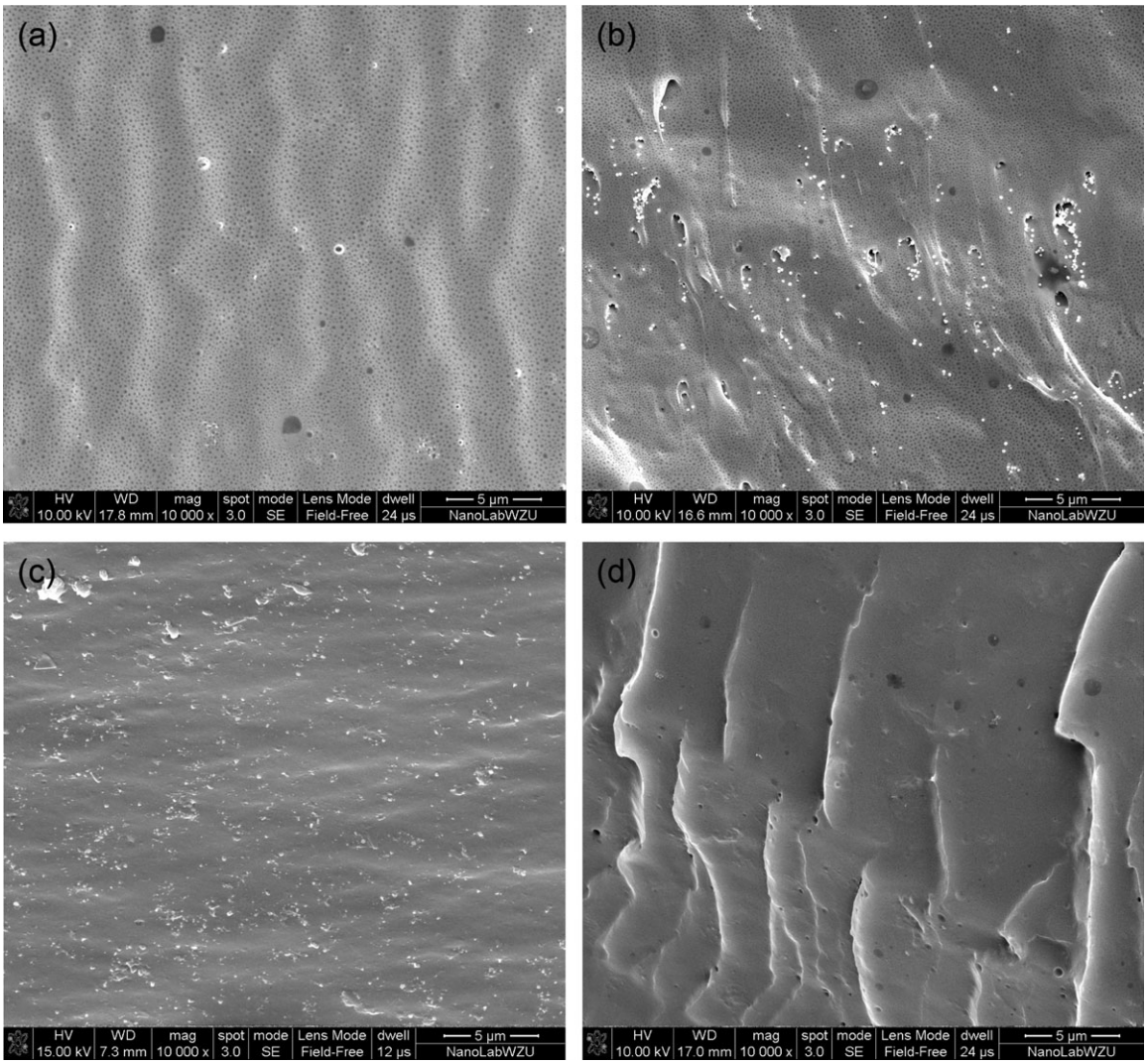

Figure 2. SEM micrographs of the fractured surfaces of (a) WPU2.5, (b) WPU5, (c) WPU10, (d) WPU0.

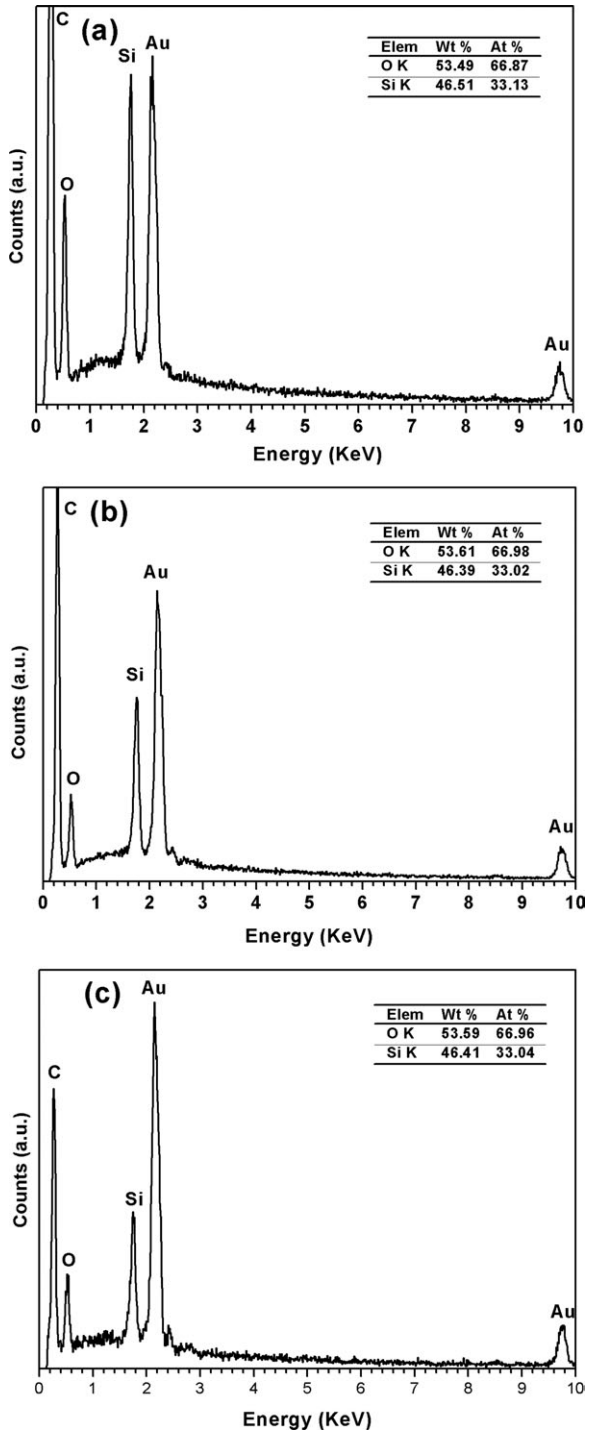

Figure 3. EDS spectrum of (a) WPU2.5, (b) WPU5, (c) WPU10.

were well dispersed in the WPU films and no phase separation appeared between the nanosilica and WPU films with the contents of TEOS increased. And the diameters of nanosilica in the hybrid films were all of about 50 nm, regardless of the TEOS contents and the resolution of TEM images. It suggested that good compatibility was achieved and the TEOS contents had little influence on the particles size and the compatibility between nanoparticles and WPU matrix. Chen et al.[13] reported that some aggregates of nanosilica in hybrid film were observed by *in situ* polymerization with commercial supplied 3 wt % nanosilica used. Chen et al.[14] also reported some aggregation of silica particles occurred with 8 wt % silica sol (66 nm) by *in situ* polymerization, which was attributed to interaction between nanosilica particles with macromolecular chains, and small numbers of polymer segments might be chemically bonded with silica particles and thus free nanosilica particles easily cause aggregation through hydrogen bonding. The dispersion of this work is different from the both, which were obviously influenced by the concentrations of nanosilica. Also, it is different from that reported by Lee et al.[8] and Bae et al,[9] who found that the average particle sizes were larger than the primary and increased with particle concentration. In this work, better dispersion implied strong interaction between nanosilica and WPU chains, and APTES bonding at the end of WPU molecule chain prevented the nanosilica from agglomerating during the synthesis of nanosilica and thus facilitated its homogeneous dispersion.

Chemical Structure Analyses

The nanosilica/WPU hybrid films were ascertained by XPS analysis (Figure 5), and the peaks corresponding to the core levels of C 1s, N 1s, O 1s, and Si 2p were identified. High-resolution spectra of Si 2p and O 1s were analyzed to verify the value states of Si and O. As shown in Figure 6, the Si—O—Si peak is located at 102.7 eV.[15] The binding energy of 101.8 eV represents the Si-alkylamine of APTES, which was functionalized onto the silica surfaces during the sol-gel process.[15] Accordingly, nanosilica in WPU is speculated to have been synthesized by *in situ* hydrolysis and condensation of TEOS and/or APTES bonding at the end of the WPU molecule chain. In addition, new chemical bonds occurred between APTES and silica nanoparticles, implying that interfacial interaction was reinforced between the organic and inorganic phases. As shown in the O1s XPS spectrum (Figure 6), the binding energy peaks located at 531.9 and 533.3 eV were assigned to —$NHCOO^-$ [16] and Si—O—Si,[17] respectively. The peak of Si—O—C at 533.1 eV[18] was covered by that of Si—O—Si, as the peaks were very near each other. The concentrations of $COO^-NR_3H^+$ and urea were so small that the peaks for COO^- and urea were ignored. These observations were consistent with the Si 2p spectrum.

The hydrolysis of TEOS and APTES, the formation of Si—O—Si by the condensation of TEOS and/or APTES, and the reaction between APTES and WPU prepolymer were further confirmed by FTIR. As shown in Figure 7(b), the NCO groups of the WPU prepolymer completely reacted with the amine groups of APTES, as evidenced by the disappearance of the peak of the NCO groups (2270 cm^{-1})[5] and the appearance of the peak of —OCH_2CH_3 in APTES (953 cm^{-1})[19] after the capping reaction of NCO groups with APTES. Moreover, Si—OH was confirmed by the peaks at 958 cm^{-1} [Figure (7c–f)], which can be attributed to the deformation vibrations of Si—OH.[20] These findings indicate that TEOS and APTES were hydrolyzed. Furthermore, Si—O—Si can be identified by the peaks at 466, 769, and 1068 cm^{-1} [Figure (7c–f)],[21–23] corresponding to the bending, symmetric stretching, and asymmetric stretching vibrations of Si—O—Si, respectively.[24] However, the peak at 1068 cm^{-1} cannot be positively identified, because it also could be attributed

Applied Polymer SCIENCE

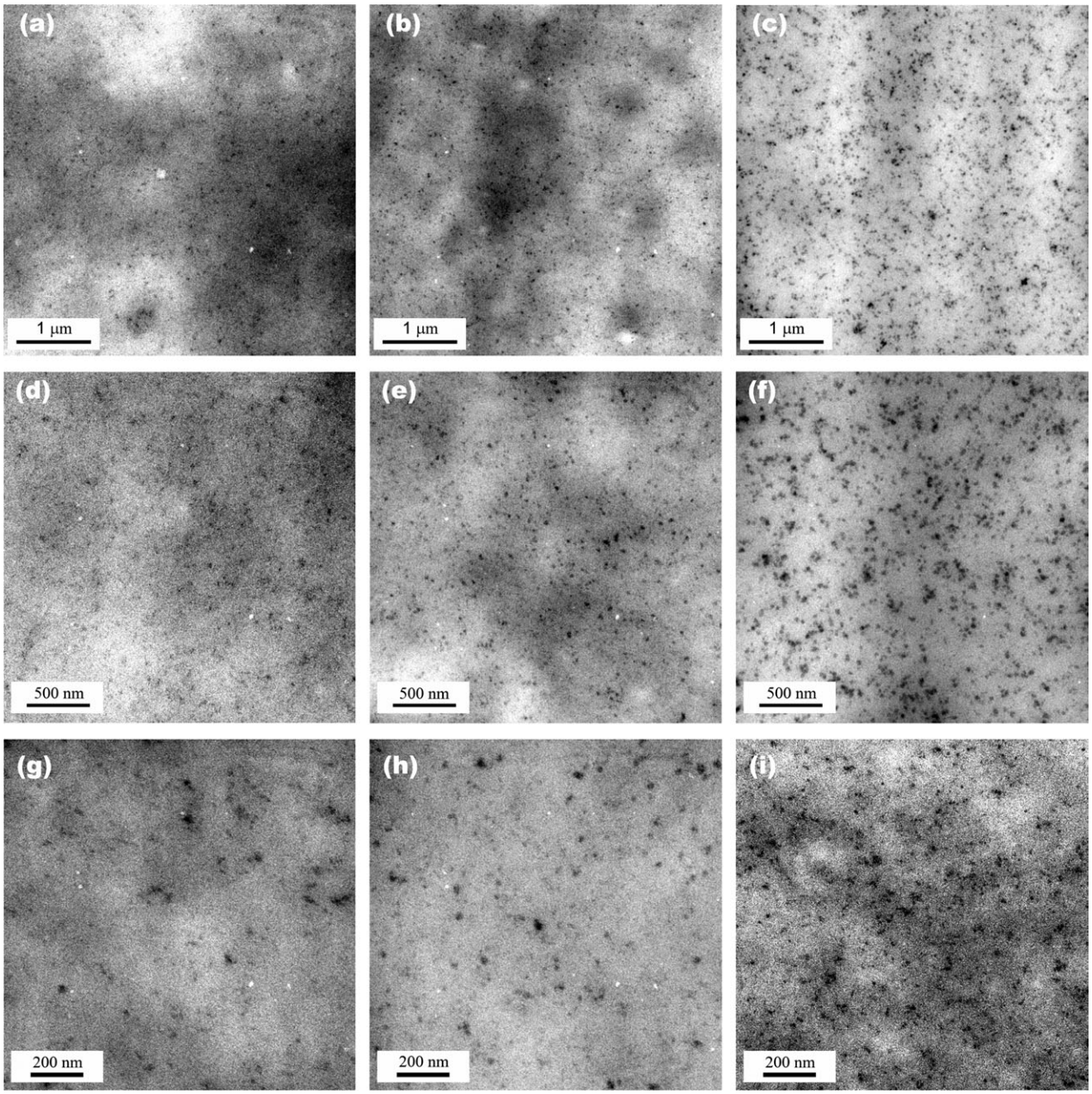

Figure 4. TEM images of nanosilica/WPU hybrid with different TEOS contents. (a), (d), (g) WPU2.5. (b), (e), (h) WPU5. (c), (f), (i) WPU10.

to either the stretching vibrations of C—C, C—O, and CH_2, or the rocking vibrations of CH_2.[25,26] As discussed above, TEOS contents (from 2.5 to 10 wt %) had no observable influence on the reaction characteristic of hybrids.

Advancing Contact Angle and Water Resistance

Advancing contact angle of water on the hybrid films shows that an increase in TEOS contents could result in an increase in contact angle, as shown in Figure 8, indicating the improved hydrophobicity of the nanosilica/WPU hybrids. This may be attributed to the siloxane units of APTES migrating to the surface of the films and the increased formation of Si—O—Si linkages (verified by XPS and FTIR) after the condensation of silanol groups.[27] The advancing contact angle decreased to 99.4° with 10 wt % TEOS from a maximum of 101.2° with 7.5 wt % TEOS, probably because the excess polar groups of uncondensated silanol lowered the hydrophobicity of the hybrids as the TEOS contents increased.

The influence of TEOS weight percentages on the water absorption of the films is shown in Figure 9. Water absorption decreased from 17.3 to 5.5% as the TEOS contents increased from 0 to 10 wt %, implying the enhancement in water resistance of nanosilica/WPU hybrids. This enhancement may be ascribed to the improved hydrophobicity of the hybrid, which was verified by advancing contact angles measured. Si—O—Si crosslinking density is also considered to be helpful for improving water resistance.[19] The decrease in water absorption was

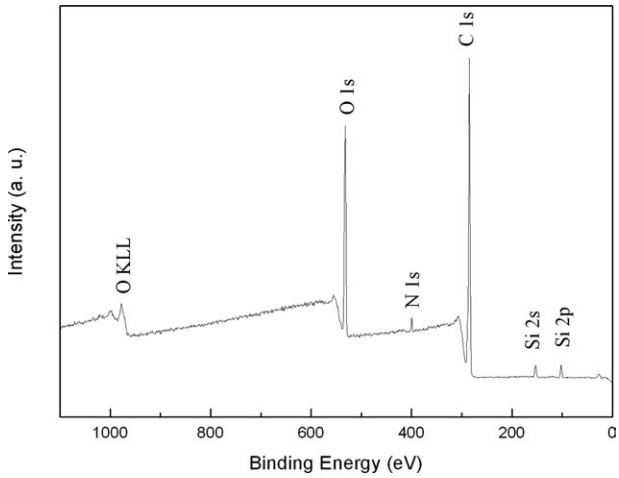

Figure 5. XPS survey spectrum of nanosilica/WPU hybrid.

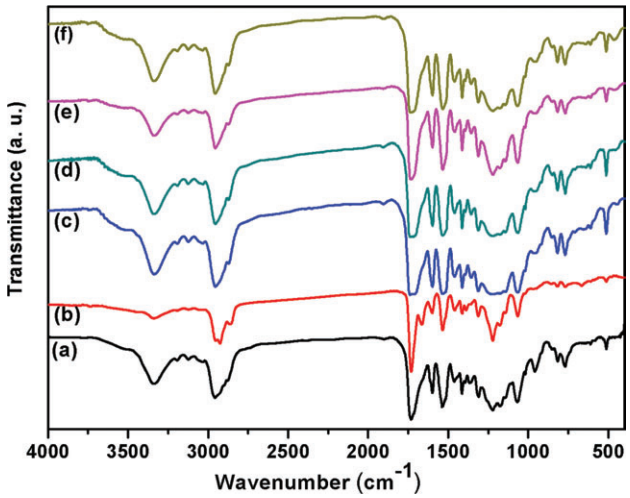

Figure 7. FTIR spectra of (a) WPU0, (b) WPU prepolymer end-capped with APTES, (c) WPU2.5, (d) WPU5, (e) WPU7.5, (f) WPU10. [Color figure can be viewed in the online issue, which is available at wileyonlinelibrary.com.]

very evident when the TEOS contents were 2.5 wt %, after which the decrease slowed down as the TEOS contents increased. The increased TEOS contents increased the possibility of the aggregation of nanoparticles, which formed porosities in the microstructure of the hybrid composites.[28] These porosities would be favorable for water absorption.[29] Consequently, the decrease in water absorption slowed down when the TEOS contents were higher than 2.5 wt %.

Jeon et al.[5] reported the water absorption decreased from 6.49 to 5.73%. In his work, two nanosilica/WPU hybrids were compared, and the hybrid having network structure by sol-gel process exhibited better water resistance, which was believed to originate from the higher Si—O—Si crosslinking density. The water absorption of the nanosilica/WPU hybrids in this study decreased about 11.8% as the TEOS contents increased from 0 to 10 wt %. It suggested that the nanosilica/WPU hybrids exhibited better water resistance than the hybrids (0.76%) synthesized by Jeon et al.[5] Chen et al.[30] compared the water absorption of the nanosilica/WPU hybrids with silica modified with four different qualitative SCA by thermogravimetric analysis. Water resistance was better in this study compare with the above, it was conclude that crosslinking density of the hybrids prepared by this method was higher than that by the methods reported by previously published work. Those suggested that

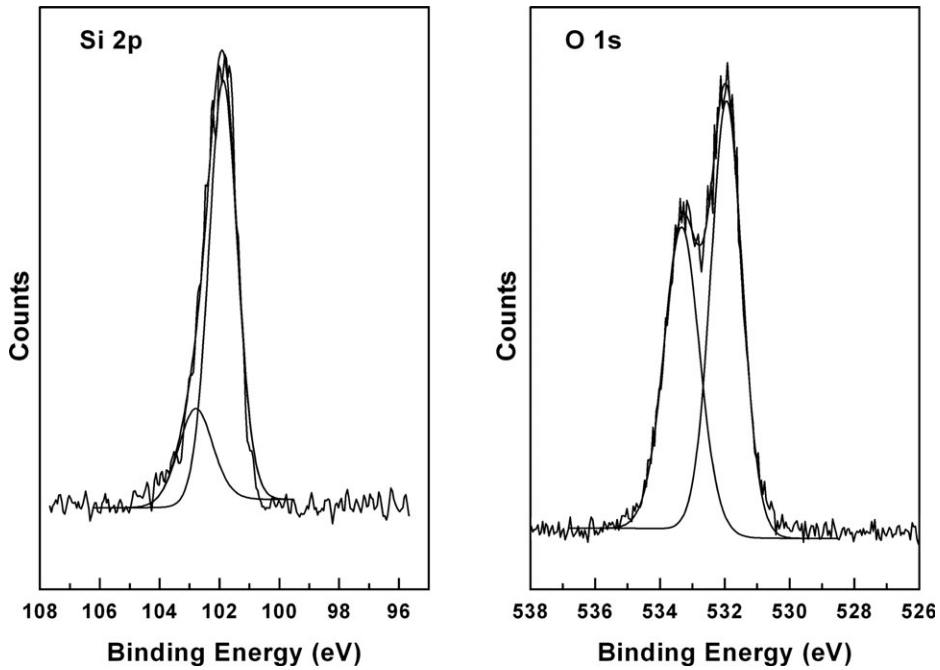

Figure 6. High-resolution of XPS analysis of nanosilica/WPU hybrid.

Applied Polymer SCIENCE

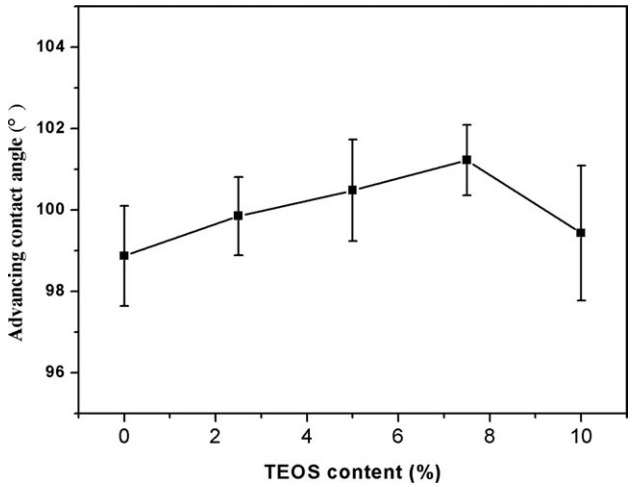

Figure 8. Advancing contact angle of nanosilica/WPU hybrid films with different TEOS contents.

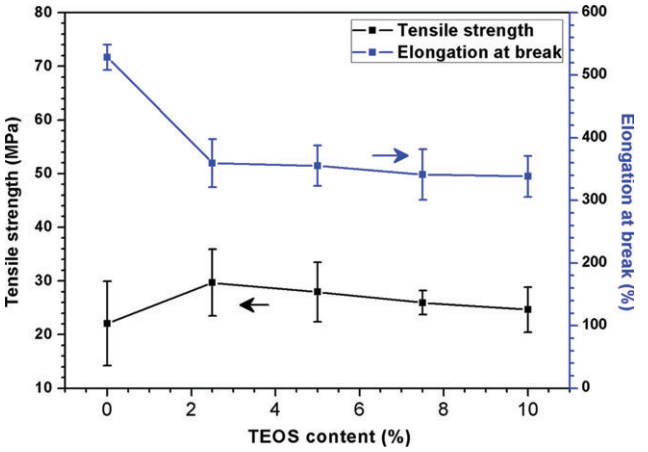

Figure 10. Effect of the TEOS contents on the mechanical properties of nanosilica/WPU hybrids. [Color figure can be viewed in the online issue, which is available at wileyonlinelibrary.com.]

the crosslinking density was higher and the chemical bonding between silica and WPU polymer molecules was stronger.

Mechanical Properties

The mechanical properties of nanosilica/WPU hybrids, including tensile strength and elongation at break were measured. Generally, the tensile strength of the nanosilica/WPU hybrids clearly increased and the elongation at break decreased with increasing TEOS contents (Figure 10). The improved tensile strength of the nanosilica/WPU hybrids may be attributed to crosslinking density,[19] the strong chemical interaction between the nanosilica surface and the WPU chains via APTES,[7] as well as the uniform nanosilica distribution in the WPU matrix,[31] which were proved by the SEM, TEM, XPS, FTIR, and water absorption results. The strong chemical interaction, certified by XPS and FTIR results, helped the transferring of the stress burdened by the WPU matrix to the rigid nanosilica. The good dispersion of silica in the WPU matrix reduced the stress concentration and enhanced the uniformity of stress distribution. As a result, good reinforcement was achieved with the homogeneous dispersion of silica in the hybrids. Moreover, the increased Si—O—Si crosslink between the polymer chains reinforced the tensile strength of the hybrids.

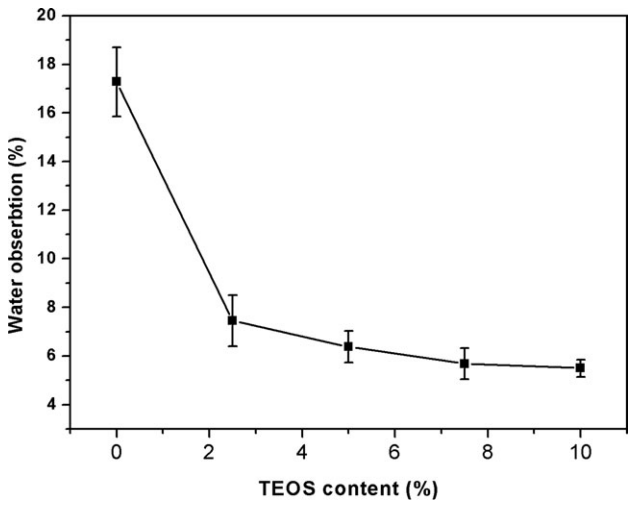

Figure 9. Influence of TEOS weight percentages on the water absorption of nanosilica/WPU hybrid films.

Better improvements in the tensile strength were obtained when the TEOS contents were less than 2.5 wt %, because both the nanosilica content and the chemical interaction between the components increased. The tensile strength increased to a maximum of 29.7 MPa with 2.5 wt % TEOS, an increase of about 34% compared with the unmodified counterpart (22.1 MPa). The improvement in tensile strength slightly decreased when the TEOS contents were higher than 2.5 wt %. This may be because the reinforcement of nanosilica was minimized by extreme differences between the WPU and nanosilica when the TEOS contents were increased. And, the chemical interaction strength between the nanosilica and WPU introduced by APTES remained unchanged as the APTES content was held constant (0.0045 mol, Table I). Thus, the slope of improvement remained constant when the TEOS contents were higher than 2.5 wt %, which is related to the invariable amount of interaction. Better dispersion and less aggregation of nanosilica synthesized *in situ* optimized nanoparticles' reinforcement. Also, chemical bonds and the higher crosslinking density are assumed to avail the reinforcement.

In contrast, elongations at break of the hybrids decreased with the addition of TEOS, and it slightly reduced when the TEOS contents were more than 2.5 wt %. It was mainly due to the chemical interaction between silica and WPU matrix and the high Si—O—Si crosslinking density formed by *in situ* hydrolysis and condensation of TEOS and APTES, which constrained the polymer chain mobility. The chemical interaction and the Si—O—Si crosslinking density were higher when TEOS was less than 2.5 wt %, so elongation at break declined more. When the content of TEOS was higher than 2.5 wt %, the chemical interaction and the crosslinking density slightly increased as the APTES content was held constant, so the elongation at break declined less. The decease feature is different from those reported by Chen et al.[32] and Wang et al.[2] Chen et al.[32] prepared acrylic based polyurethane/silica composites, which embedded

with different methyltriethoxylsilane modifying silica content. In that case, elongation at break slightly reduced when the silica content was more than 6 wt %, which was probably because of the stronger interfacial interaction at higher silica concentration. Wang et al.[2] reported that elongations at break decreased 93% and the reason was not mentioned. Also, the mechanical properties are different from those of nanosilica/WPU hybrids.[5] The tensile strength improvement (34%) and elongations at break decrease (191%) in this study was higher than those reported by Jeon et al.[5] In their work, polyurethane was end-capped by APTES and reacted with silica particles through sol-gel process. It was reported by them that the reason for tensile strength increase and elongation at break decrease was due to chemical bonding, fillers reinforcement, and crosslink formations between WPU and silica. Compared the mechanical properties variation with that of the above, it was suspected that chemical bonding and the crosslinking density of the hybrids in this study were higher than the hybrids reported by them.

DSC was used to measure the glass transition temperature (T_g) and further understand the interaction between nanosilica and the WPU matrix (Figure 11). The soft-segment T_g values are tabulated in Table II. The soft-segment T_g of the nanosilica/WPU hybrids showed a tendency to decrease. It reached −42.3°C when the TEOS contents were 2.5 wt % and then gradually increased to −39.3°C as the TEOS contents increased to 10 wt %. The presence of flexible Si—O—Si linkages acting as plasticizers may contribute toward lowering the soft-segment T_g. Moreover, the chemical interaction between the nanosilica and WPU introduced by APTES decreased the interaction between soft and hard segments by shielding the hard segment from binding with the soft one, thereby reducing their physical crosslinkages. As a result, the soft-segment T_g of the nanosilica/WPU hybrids decreased with TEOS loading. This T_g feature is much different from that of nanosilica/WPU hybrids reported by Wang et al.,[2] which were virtually unchanged with the increasing content of silica. In Wang's study, the weak electrostatic interactions between silica and WPU cannot significantly influence the segmental motion, thus the silica/WPU hybrid films had similar values of T_g's. From the comparison, it can be concluded that the chemical interaction between the nanosilica and WPU formed by this method was stronger than that by the method Wang adopted. When the TEOS contents were higher than 2.5 wt %, the soft-segment T_g was gradually enhanced but remained lower than that of WPU. The effect of the shield may have weakened when the concentration of TEOS increased because the increased amount of nanosilica was unable to chemically interact with WPU. The variation tendency is in good agreement with the mechanical property results.

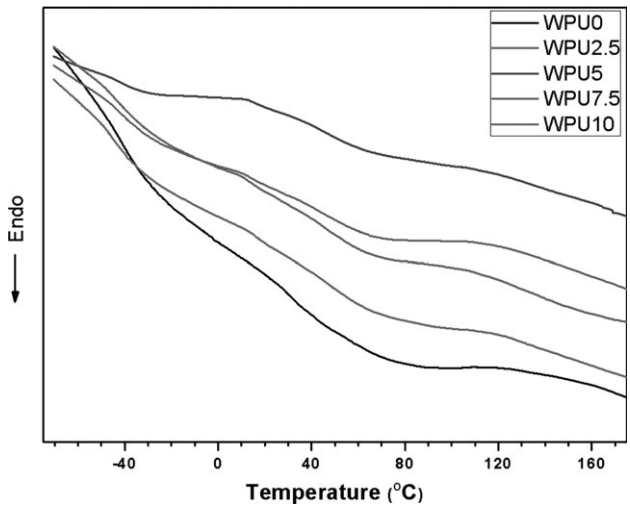

Figure 11. DSC thermograms of nanosilica/WPU hybrids with different TEOS contents. [Color figure can be viewed in the online issue, which is available at wileyonlinelibrary.com.]

Table II. Glass Transition Temperature of Nanosilica/WPU Hybrids with Different TEOS Contents

TEOS contents/wt %	0	2.5	5	7.5	10
T_g/°C	−39.4	−42.3	−41.9	−40.6	−39.3

CONCLUSIONS

A homogenous nanosilica/WPU hybrid was synthesized by *in situ* hydrolysis and condensation of TEOS and APTES using a sol-gel method. In the hybrids, the nanosilica was approximately 50 nm in diameter. SEM, EDS, TEM, XPS, and FTIR analyses showed that APTES underwent both a reaction with the isocyanate group (NCO group) of the WPU prepolymer and a sol-gel process with TEOS to form a hybrid via covalent bonds. These results suggested that the dispersion of nanosilica in WPU and the compatibility between nanosilica and WPU were improved by APTES. The hydrophobicity, water resistance, and tensile strength of the nanosilica/WPU hybrid were increased while its elongation at break and T_g decreased. These results also implied chemical bonds and high crosslinking density between nanosilica and WPU was obtained. Therefore, a synergetic combination of the properties of each of the constituents was achieved.

ACKNOWLEDGMENTS

The authors would like to thank the financial support of the Science and Technology Project of Wenzhou (G20100074), this work was also supported by the Foundation of Zhejiang Educational Committee (Y201016832).

REFERENCES

1. Yang, C. H.; Yang, H. J.; Wen, T. C.; Wu, M. S.; Chang, J. S. *Polymer* **1999,** *40*, 871.
2. Wang, L.; Shen, Y.; Lai, X.; Li, Z. *J. Appl. Polym. Sci.* **2011,** *119*, 3521.
3. Yeh, J. M.; Yao, C. T.; Hsieh, C. F.; Yang, H. C.; Wu, C. P. *Eur. Polym. J.* **2008,** *44*, 2777.
4. Sardon, H.; Irusta, L.; Fernández-Berridi, M. J.; Lansalot, M.; Bourgeat-Lami, E. *Polymer* **2010,** *51*, 5051.
5. Jeon, H. T.; Jang, M. K.; Kim, B. K.; Kim, K. H. *Colloids Surf. A* **2007,** *302*, 559.

6. Schadler, L. S.; Kumar, S. K.; Benicewicz, B. C.; Lewis, S. L.; Harton, S. E. *MRS Bull.* **2007,** *32*, 335.
7. Zou, H.; Wu, S.; Shen, J. *Chem. Rev.* **2008,** *108*, 3893.
8. Lee, S. K.; Yoon, S. H.; Chung, I.; Hartwig, A.; Kim, B. K. Handbook of X-ray Photoelectron Spectroscopy. *J. Polym. Sci. Part A: Polym. Chem.* **2011,** *49*, 634.
9. Bae, C.; Park, J.; Kim, E.; Kang, Y.; Kim, B. *J. Mater. Chem.* **2011,** *21*, 11288.
10. Chen, J.; Zhou, Y.; Nan, Q.; Sun, Y.; Ye, X.; Wang, Z. *Appl. Surf. Sci.* **2007,** *253*, 9154.
11. Schubert, U.; Huesing, N.; Lorenz, A. *Chem. Mater.* **1995,** *7*, 2010.
12. Judeinstein, P.; Sanchez, C. *J. Mater. Chem.* **1996,** *6*, 511.
13. Chen, X.; Wu, L.; Zhou, S.; You, B. *Polym. Int.* **2003,** *52*, 993.
14. Chen, Y.; Zhou, S.; Yang, H.; Gu, G.; Wu, L. *J. Colloid Interface Sci.* **2004,** *279*, 370.
15. Phonthamachai, N.; Chia, H.; Li, X.; Wang, F.; Tjiu, W. W.; He, C. *Polymer* **2010,** *51*, 5377.
16. Beamson, G.; Briggs, D. High Resolution XPS of Organic Polymers: the Scienta ESCA300 Database; Wiley: Chichester, UK, **1992.**
17. Moulder, J.; Stickle, W.; Sobol, P.; Bomben, K. Handbook of X-ray Photoelectron Spectroscopy. Perkin-Elmer Corporation: Eden Prairie, MN, 1992.
18. Hammer, P.; Schiavetto, M.; dos Santos, F.; Benedetti, A.; Pulcinelli, S.; Santilli, C. *J. Non-Cryst. Solids* **2010,** *356*, 2606.
19. Lai, X.; Li, X.; Wang, L.; Shen, Y. *Polym. Bull.* **2010,** *65*, 45.
20. Sassi, Z.; Bureau, J.; Bakkali, A. *Vib. Spectrosc.* **2002,** *28*, 299.
21. Ramamoorthy, A.; Rahman, M.; Mooney, D. A.; Don MacElroy, J. M.; Dowling, D. P. *Surf. Coat. Technol.* **2008,** *202*, 4130.
22. Ouyang, M.; Klemchuk, P. P.; Koberstein, J. T. *Polym. Degrad. Stab.* **2000,** *70*, 217.
23. Kim, J. M.; Chang, S. M.; Kong, S. M.; Kim, K. S.; Kim, J. S.; Kim, W. S. *Ceram. Int.* **2009,** *35*, 1015.
24. Chan, C. K.; Chu, I. *Polymer* **2001,** *42*, 6089.
25. Sim, L. H.; Gan, S. N.; Chan, C. H.; Yahya, R. *Spectrochim. Acta A* **2010,** *76*, 287.
26. Huang, L.; Zhai, M.; Peng, J.; Xu, L.; Li, J.; Wei, G. *J. Colloid Interface Sci.* **2007,** *316*, 398.
27. Florian, P.; Jena, K. K.; Allauddin, S.; Narayan, R.; Raju, K. *Ind. Eng. Chem. Res.* **2010,** *49*, 4517.
28. Santos, C.; Clarke, R. L.; Braden, M.; Guitian, F.; Davy, K. W. M. *Biomaterials* **2002,** *23*, 1897.
29. Zhao, C. X.; Zhang, W. D. *Eur. Polym. J.* **2008,** *44*, 1988.
30. Chen, G.; Zhou, S.; Gu, G.; Yang, H.; Wu, L. *J. Colloid Interface Sci.* **2005,** *281*, 339.
31. Subramani, S.; Choi, S. W.; Lee, J. Y.; Kim, J. H. *Polymer* **2007,** *48*, 4691.
32. Chen, G.; Zhou, S.; Gu, G.; Wu, L. *Colloids Surf. A* **2007,** *296*, 29.